Available online at www.sciencedirect.com
SCIENCE DIRECT
Combustion and Flame 141 (2005) 22–39
Combustion and Flame
www.elsevier.com/locate/combustflame

Mechanism and modeling of the formation of gaseous alkali sulfates

Peter Glarborg [a,*], Paul Marshall [b]

[a] Department of Chemical Engineering, Technical University of Denmark, 2800 Lyngby, Denmark
[b] Department of Chemistry, University of North Texas, P.O. Box 305070, Denton, TX 76203-5070, USA

Received 24 May 2004; received in revised form 9 July 2004; accepted 18 August 2004

Available online 13 October 2004

Abstract

The formation of gaseous alkali sulfates is known to yield aerosols and may also contribute to deposition and corrosion in the combustion of solid fuels such as biomass. In the present work a model for the gaseous sulfation of alkali hydroxide (*A*OH) and alkali chloride (*A*Cl) is developed. It relies on a detailed chemical kinetic model for the high-temperature gas-phase interaction between alkali metals, the O/H radical pool, and chlorine/sulfur species. Thermodynamic properties of a number of potassium and sodium species have been estimated from Gaussian 3 ab initio calculations. Particular attention is paid to alkali hydrogen sulfates and alkali oxysulfur chlorides as potential gas-phase precursors of A_2SO_4. Rate constants have been drawn from the literature, from analogy with known reactions, or from QRRK theory. A detailed reaction mechanism for sulfation is proposed. The alkali transformations proceed by a number of molecule–molecule reactions, which can be expected to exhibit ionic behavior. The sulfation is initiated by oxidation of SO_2 to SO_3. Sulfur trioxide subsequently recombines rapidly with *A*OH or *A*Cl to form an alkali hydrogen sulfate, $AHSO_4$, or an alkali oxysulfur chloride, ASO_3Cl. According to the present work, both of these complexes are sufficiently stable in the gas phase to act as precursors for alkali sulfate. Alkali hydrogen sulfate and alkali oxysulfur chloride are subsequently converted to alkali sulfate in fast shuffle reactions such as $ASO_3Cl + H_2O \rightarrow AHSO_4 + HCl$ and $AHSO_4 + ACl \rightarrow A_2SO_4 + HCl$. Modeling predictions compare favorably with the experimental results of K. Iisa et al. [Energy Fuels 13 (1999) 1184–1190] on the gas-phase sulfation of potassium chloride at 1373 K. They investigated the degree of sulfation of KCl in a gaseous mixture of $SO_2 + O_2 + H_2O + N_2$ as a function of reaction time and gas composition in an entrained flow reactor. The modeling predictions are not sensitive to the estimated properties in the alkali subset (thermodynamic data, rate constants) within the assigned error limits; the predicted degree of sulfation is influenced mainly by the rate of oxidation of SO_2 and the production of chain carriers in the system.

Keywords: Alkali metals; Sulfation; Aerosol formation; Chemical kinetics; Thermodynamic properties

1. Introduction

Interest in the high-temperature gas-phase chemistry of alkali metals has been motivated by its importance for flame inhibition [1–6], for deposition and

* Corresponding author.
E-mail address: pgl@kt.dtu.dk (P. Glarborg).

0010-2180/$ – see front matter
doi:10.1016/j.combustflame.2004.08.014

corrosion in naval engines and gas turbines [7–12] and in the combustion of solid fuels such as biomass [13–16], coal [17–20], and black liquor [21–23], for in-furnace NO_x control [24–27], and for aerosol formation in biomass combustion [28–30]. Over the last two decades, understanding of the thermodynamic properties of alkali metals and of their reaction chemistry has improved significantly. Recent progress in thermochemistry has relied mostly on ab initio calculations [31–42], while results on elementary reactions largely have been experimental, facilitated by the development of powerful experimental techniques [43,44]. Most of the work on reaction rates has been motivated by interest in atmospheric chemistry and was conducted at low temperature, but for a number of reactions data are also available at higher temperatures. However, despite extensive research in the past, important aspects of the chemistry of sodium and potassium are still unresolved. Alkali metals are difficult to deal with both theoretically and experimentally, and the thermochemistry for many alkali species, as well as reaction rates for potentially important reactions, is uncertain or even unavailable.

Attempts to develop detailed reaction mechanisms for the chemistry of K and Na have been limited in the past. Steinberg and co-workers [11,45,46] developed the first detailed mechanisms for alkali chemistry in flames, focusing on alkali atom removal, catalyzed radical recombination, and Na/S interactions important for deposition and corrosion. This early effort has formed the basis of subsequent mechanistic studies on sodium transformations in coal combustion [19] and on the effect of potassium additives on gun muzzle flash [6]. More recent kinetic efforts have focused on predicting the effect of alkali metals on NO_x control technologies such as selective noncatalytic reduction of NO, N_2O removal, and reburning [24–27].

The objectives of the present work are partly to update the thermochemistry and high-temperature gas-phase reaction mechanisms of sodium and potassium and partly to identify a plausible mechanism for the formation of gas-phase A_2SO_4 (A = K or Na). Alkali sulfates are important for aerosol formation and deposition/corrosion in systems such as biomass combustion, where sulfur, chlorine, and alkali metals may interact. However, the formation mechanism for these sulfates is still in dispute, and until recently it has been questioned whether they are formed at all in the gas phase in combustion systems. Particular attention in the present work is paid to the importance of alkali hydrogen sulfates as gas-phase precursors of A_2SO_4. To determine the thermal stability of $KHSO_4$ and $NaHSO_4$ we have estimated their thermodynamic properties from ab initio computations. Also, chlorinated intermediates are considered. A chemical kinetic model for formation of K_2SO_4 is proposed and modeling predictions are compared with data from entrained-flow reactor experiments [47].

2. Formation of alkali sulfates

Most previous work on alkali sulfate formation has been motivated by the problems with deposition and corrosion in combustion systems [19]; alkali sulfates are known to be very active corrosion agents. The mechanism of formation of condensed or solid alkali sulfates in deposits has long been in dispute. Both homogeneous [7,9,10] and heterogeneous [11,12,19,46,48,49] mechanisms have been advocated in the literature. The homogeneous mechanism involves formation of an alkali sulfate in the gas phase, followed by condensation onto a surface. In the heterogeneous mechanism, a gas-phase alkali-containing precursor is transported to the surface, where it is sulfated by reactions in condensed or solid phase. Even though gaseous K_2SO_4 [18,50,51] and Na_2SO_4 [52–55] have been shown in vaporization experiments to be stable at moderate to high temperatures, it has been questioned [11,12,46] whether they are formed in combustion systems. Gaseous Na_2SO_4 has been detected by mass spectrometry in the postflame zone of a CH_4/O_2 flame doped with SO_2 and NaCl [8] and in black liquor combustion experiments [21,56], but such measurements may be affected by a deposit forming around the sampling orifice [46].

Experiments with sodium and potassium salt deposition in flames [12,49] support a heterogeneous formation mechanism for alkali sulfate deposits. Sulfation of solid-phase alkali chloride has been studied both experimentally [10,22,57–60] and theoretically [61,62]. Below 900 K the sulfation is a slow, low-activation-energy reaction [10,22,57,60], but above this temperature a sharp increase in the rate constant is observed [58,60]. The apparent shift in mechanism may be caused by the presence of molten sodium chloride; mixtures of Na_2SO_4 + NaCl form a melt in this temperature range. The heterogeneous sulfation reaction is promoted in the presence of SO_3 [10,59,62]. The reaction between NaCl(s), SO_3, and H_2O proceeds without an activation barrier, according to experimental results and molecular orbital calculations [62]. The mechanism is believed to involve the formation of sodium hydrogen sulfate, which then reacts with solid sodium chloride, forming sodium sulfate in two steps: $H_2SO_4 + NaCl(s) \rightarrow NaHSO_4(s) + HCl$, $NaHSO_4(s) + NaCl(s) \rightarrow Na_2SO_4(s) + HCl$. Less is known about sulfation of molten alkali chloride, but even in the presence of SO_3, it is a comparatively slow process [47].

The importance of alkali sulfates for submicron particle formation has been recognized only recently

[23,28–30]. Contrary to formation of deposits, which may develop over long times, only a few seconds of reaction time are available for aerosol formation. Extrapolation of the results for heterogeneous sulfation [47,58,60] indicates that even at high temperatures, the sulfation of solid and molten alkali chloride by SO_2, H_2O, and O_2 is too slow to play an important role on short time scales. The detection of alkali sulfate aerosols in biomass combustion [28,29,63] and in flow reactors [30,47] supports the existence of a gas-phase mechanism. Based on a theoretical analysis of the measured concentration of submicron particles in biomass combustion, Christensen et al. [29] concluded that the gas-to-particle conversion occurs by the homogeneous nucleation of K_2SO_4 particles, which act as condensation nuclei for the subsequent condensation of KCl. This interpretation is supported by observations on aerosol formation from alkali chloride in flow reactors. Jensen et al. [30] analyzed aerosol formation during cooling of a synthetic flue gas ($O_2/H_2O/N_2$) with sodium or potassium vapors in a laboratory flow reactor. In both the absence and the presence of a small number of particles (to suppress alkali chloride nucleation), addition of SO_2 to the feed gas led to a remarkable increase in the number concentration of effluent particles and caused their composition to include sulfate in addition to chloride. The results show that alkali sulfates can be formed by the sulfation of vapor-phase chloride and point to homogeneous nucleation as the source of alkali sulfate aerosols. The entrained flow reactor experiments of Iisa et al. [47], which are discussed in greater detail below, support the interpretation that alkali sulfate aerosols are formed by the sulfation of vapor-phase rather than solid or molten alkali chloride.

To understand how alkali sulfates can be formed in the gas phase, it is instructive to look at the reactivity of gaseous alkali species. Many alkali compounds, for instance, alkaline hydroxides and halides, are polar species and exhibit strongly ionic behavior; i.e., they act similarly to gas-phase ions. Due to attractive forces between the reactants, a number of reactions involving alkali species are extremely fast. For molecule–molecule reactions this is typically caused by a significant dipole–dipole-induced dipole moment, while atom–diatom reactions may involve an electron transfer mechanism, which induces a switch from a neutral to an attractive ionic potential energy surface when the reactants approach each other [64].

Ionic behavior has been observed for association reactions involving, for instance, NaO or NaOH. Reactions of these alkaline species with stable molecules such as CO_2 and O_2 proceed at rates similar to those of ion–molecule reactions [65]. For instance, the reactivity of sodium hydroxide resembles that of the corresponding negative ion, OH^-, and the two reactions $NaOH + CO_2 + M = NaHCO_3 + M$ and $OH^- + CO_2 + M = HCO_3^- + M$ have rate constants that agree within a factor of 2 [65]. The ionic behavior is also pronounced for reactions of alkaline halides with other alkaline halides or hydrogen halides. Molecular beam scattering experiments indicate that these reactions involve a strong collision complex [66] and can be expected to be fast. This has been confirmed for dimerization reactions involving alkaline halides [67], but a number of reactions, where the collision complex dissociates to products, behave similarly. An interesting example is the exothermic reaction between sodium hydroxide and hydrogen chloride,

$$NaOH + HCl \rightarrow NaCl + H_2O. \qquad \text{(R36)}$$

The reaction number refers to the mechanism listed in Appendix B, which is discussed below. Both reactants in this reaction are stable molecules and HCl has a strong covalent bond. For these reasons, the reaction would be expected to be slow and have a significant barrier, despite its exothermicity. However, measurement of k_{36} at 308 K indicates a value close to the gas kinetic limit [68]. Similar behavior is observed for other four-centered reactions, such as $CsCl + KI \rightarrow CsI + KCl$, which proceeds without any activation energy and has a large cross section [69].

The existence of a class of very fast alkali reactions between stable molecules has implications for the formation of gaseous alkali sulfate: a mechanism involving only stable precursors is plausible. The first step appears to be oxidation of SO_2 to SO_3, which has been shown to be rate-limiting [29,47]. The subsequent step is most likely an association reaction involving alkali hydroxide or alkali chloride (the most abundant alkali species in combustion gases) with SO_3:

$$AOH + SO_3(+M) = AHSO_4(+M), \qquad \text{(R44/93)}$$

$$ACl + SO_3(+M) = ASO_3Cl(+M). \qquad \text{(R53/102)}$$

If the complexes formed in these reactions, alkali hydrogen sulfate and an alkali oxysulfur chloride, are sufficiently stable at high temperatures, they may conceivably participate in a series of shuffle reactions ultimately leading to the formation of alkali sulfate:

$$ASO_3Cl + H_2O = AHSO_4 + HCl, \qquad \text{(R55/104)}$$

$$ASO_3Cl + AOH = A_2SO_4 + HCl, \qquad \text{(R56/105)}$$

$$AHSO_4 + AOH = A_2SO_4 + H_2O, \qquad \text{(R51/100)}$$

$$AHSO_4 + ACl = A_2SO_4 + HCl. \qquad \text{(R52/101)}$$

The association reactions (R44/93) and (R53/102) resemble the recombination of NaOH with CO_2 discussed above and can be expected to have comparable rate constants, at least at the high-pressure limit.

Also, the shuffle reactions can be expected to be fast by analogy with other reactions involving alkaline halides and hydrogen halides, for instance, (R36).

The proposed mechanism indicates a fast and efficient gas-phase sulfation process, with oxidation of SO_2, rather than alkali transformations, being rate-limiting. This is in agreement with experimental observations from short-residence-time experiments in flames and flow reactors. Alkali sulfation is known to be fast, occurring in a few milliseconds during cooling in a postflame environment [7,8]. It is efficient in sulfating KCl [47] and it proceeds at temperatures as low as 1085 K [29,30]; below this temperature the conversion of SO_2 to SO_3 becomes very slow. The mechanism relies on stable alkali precursors, in agreement with the observation that pathways involving alkali radicals such as ASO_2 and A_2SO_3 yield insignificant amounts of sulfate [11]. It is also noteworthy that the proposed gas-phase mechanism has some resemblance to the mechanism derived for sulfation of solid sodium chloride at 873 K [62]. Both mechanisms involve the formation of SO_3 as a first step, followed by a sequence of reactions between stable species. While hydrogen sulfate, due to its low thermal stability in the gas phase, is not important in the homogeneous mechanism, both schemes involve an alkaline hydrogen sulfate as an intermediate, in either solid or gaseous form.

The plausibility of the proposed gas-phase mechanism depends on the thermal stability of the alkaline hydrogen sulfates and the alkaline oxysulfur chlorides in the gas phase. To our knowledge these complexes have not previously been detected in the gas phase, and no data are available on their thermochemistry. In the present work we estimate the thermodynamic properties of $NaHSO_4$, $KHSO_4$, $NaSO_3Cl$, and KSO_3Cl as described in the following section. Based on these results and a detailed reaction mechanism for the K/Na/S/Cl chemistry, we then evaluate the proposed mechanism by comparing modeling predictions with available experimental results for potassium sulfate formation.

3. Thermodynamic properties of potential alkali sulfate precursors

The experimental database for gas-phase alkali metal–sulfur species is sparse and is augmented here by results from ab initio calculations made with the Gaussian 98 and 03 program suites [70,71]. Polar metallic species are a challenge for standard computational approaches [42]. We have selected G3 theory [72], as modified by Curtiss et al. [73], as our model chemistry for alkali metal compounds. Our choice is based on the availability for third- as well as second-row elements, notably potassium here, and the expansion of the valence electron space in the correlation treatment to include $2s$ and $2p$ orbitals for Na and $3s$ and $3p$ orbitals for K. This change should improve accuracy for the largely ionic species considered here (Mulliken charges on the metal atoms are typically +0.7 to 0.8), and core–valence correlation is in part taken into account as well. The G3 model chemistry relies on a series of additive calculations to approximate the QCISD(T)/G3 Large energy, where all electrons are correlated. G3 Large corresponds to a contraction of a $13s9p$ basis set to $6s5p$ for Na, augmented with diffuse, $3d2f$, and tight d and f functions. The basis set for K is a $15s13p5d$ basis contracted to $8s7p3d$, similarly augmented [73]. In G3 theory zero-point vibrational energy corrections are derived at the HF/6-31G(d) level of theory, with frequencies scaled by a standard factor of 0.8923. This correction is combined with ab initio energy changes at 0 K for a variety of working reactions outlined below, to obtain ΔH_0. For the atoms H, O, Na, S, and Cl, 6-31G(d) here refers to the basis sets of Hariharan and Pople [74] and Francl et al. [75], while for K this is the basis set recently defined by Rassolov et al. [76] (which differs from that included in the Gaussian program suites). Geometries at the MP2/6-31G(d) level of theory, obtained with all electrons included in the correlation treatment, were employed for the subsequent high-level energy calculations [72]. Table 1 summarizes the G3 energies obtained, and the molecular structures of KSO_3, K_2SO_4, $KHSO_4$, and KSO_3Cl are shown in Fig. 1.

Molecular entropies, heat capacities, and temperature dependence of the enthalpies were derived from structures and vibrational frequencies. We have assumed harmonic behavior for every vibrational mode. Where literature data were unavailable, we employed unscaled frequencies and geometries obtained at the B3LYP/6-311G(d, p) level of hybrid density functional theory (see Table 1). For all the alkaline metal–oxysulfur molecules we find that in the lowest energy the cation binds to a pair of O atoms in pyramidal SO_3^- or tetrahedral SO_4^{2-}, in a similar way as found earlier for $NaSO_2$ and KSO_2, i.e., in a planar AO_2S unit [34,77].

One example validates the thermodynamic approaches used here. Use of G3 energies to obtain $\Delta_f H_0(NaSO_2)$ via the dissociation process,

$$NaSO_2 \rightarrow Na + SO_2, \qquad (a)$$

avoids consideration of S–O bond dissociation, which is difficult to describe accurately at moderate levels of theory [78]. The result from reaction (a) is a bond dissociation enthalpy of 205.3 kJ mol^{-1} and $\Delta_f H_0$ of

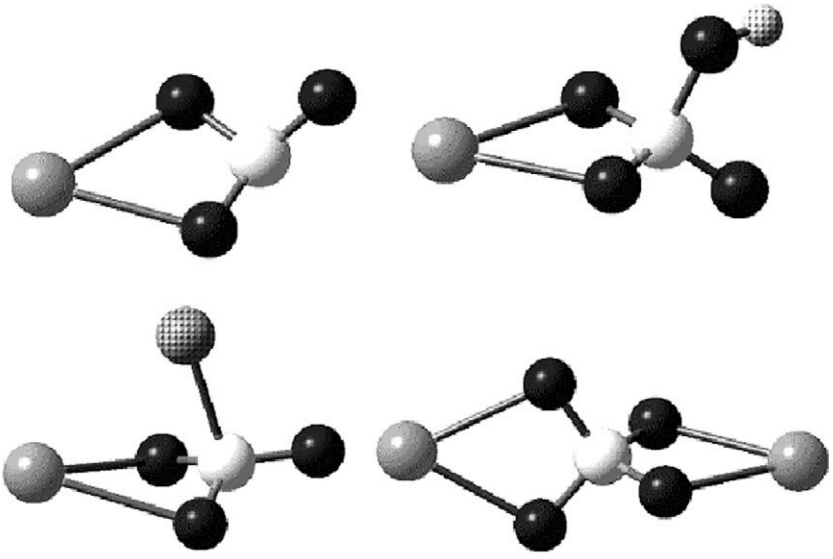

Fig. 1. Structures of (clockwise from top left) KSO_3, $KHSO_4$, K_2SO_4, and KSO_3Cl at the B3LYP/6-311G(d, p) level of theory. O atoms are shown in black, S atoms in white, and K atoms in gray. The small and large textured atoms are H and Cl, respectively.

Table 1
G3 energies, heats of formation, symmetries, inertia products and vibrational frequencies for alkali species in the Gaussian 3 calculations

Molecule	G3 energy (au)[a]	H_f^{298} (kJ mol^{-1})	Symmetry	Inertia product (GHz^3)	Vibrational frequencies (cm^{-1})
Na (ref.)	−162.12981	107.3			
K (ref.)	−599.73046	89.0			
$NaSO_2$ (ref.)	−710.62973	−381.7	C_{2V}	166.2	169, 270, 322, 535, 944, 978
KSO_2 (ref.)	−1148.23150	−399.4	C_{2V}	60.24	129, 213, 247, 497, 945, 984
Na_2SO_4 (ref.)	−1023.28883	−1033.6	D_{2d}	7.032	65(2), 269(2), 273, 360, 375, 524, 573(2), 632, 899, 1046(2), 1095
K_2SO_4 (ref.)	−1898.49164	−1094.1	D_{2d}	1.998	42(2), 201, 215(2), 285, 387, 494, 578(2), 616, 908, 1057(2), 1095
$NaSO_3$	−785.81122	−538.3[b]	Cs	58.13	103, 239, 312, 440, 506, 563, 903, 986, 1132
KSO_3	−1223.41596	−563.9[b]	Cs	23.46	76, 192, 236, 441, 493, 557, 913, 1002, 1127
$NaHSO_4$	−861.65045	−905.8[b]	Cs	21.84	79, 180, 232, 300, 362, 434, 537, 544, 586, 767, 995, 1100, 1154, 1297, 3796
$KHSO_4$	−1299.25538	−945.2[b]	Cs	9.408	56, 168, 184, 230, 366, 423, 538, 545, 572, 759, 1003, 1114, 1160, 1293, 3800
$NaSO_3Cl$	−1245.91686	−742.7[b]	Cs	7.975	60, 210, 255, 274, 316, 348, 507, 558, 594, 979, 1128, 1306
KSO_3Cl	−1683.52450	−788.6[b]	Cs	4.446	69, 99, 198, 248, 270, 283, 495, 531, 547, 991, 1196, 1328

[a] Atomic units. 1 au = 2625.5 kJ mol^{-1}.
[b] Enthalpy of formation derived from reference species as discussed in the text.

−392.1 kJ mol^{-1}. A more accurate result is expected from consideration of

$$NaSO_2 \rightarrow Na^+ + SO_2^-, \qquad \text{(b)}$$

because the molecule is ionic and this second process minimizes changes in electron configuration. The computed dissociation energy to ions is 584.2 kJ mol^{-1} which, together with experimental data for the ionization energy of Na and the electron affinity of SO_2 [79], implies a ΔH_0 for reaction (a) of 195.2 kJ mol^{-1} and $\Delta_f H_0$ of −382.0 kJ mol^{-1}. For comparison, two prior estimates of the dissociation enthalpy of $NaSO_2$ are 190 ± 15 kJ mol^{-1}, based on RRKM analysis of the reverse kinetics of reac-

tion (a) [80], and 210 ± 20 kJ mol^{-1}, derived from flame modeling [46]. It may be seen that, with appropriate choices of working reactions, G3 results yield usefully accurate thermochemistry. Here we choose isogyric processes, so that conservation of electron spin exactly cancels the influence of the empirical "higher-level correction" terms within G3 theory.

The thermochemistry of $NaHSO_4$ is derived via the isodesmic reaction

$$H_2SO_4 + Na_2SO_4 \rightarrow 2NaHSO_4, \qquad (c)$$

where $\Delta_f H$ for the reactants is known [81]. Errors arising from finite basis sets and incomplete treatment of electron correlation tend to cancel, and the main uncertainty for $NaHSO_4$ arises from the experimental input data for Na_2SO_4. The potassium analog is used for $KHSO_4$. Alkali metal atom adducts with SO_3 are characterized via the exchange

$$SO_3 + NaSO_2 \rightarrow SO_2 + NaSO_3, \qquad (d)$$

where experimental data are available for all species except $NaSO_3$. The reaction conserves the Na–O binding interaction. We also investigated the dissociation of this adduct to NaO + SO_2 and found there was no barrier beyond the endothermicity. For $NaSO_3Cl$ we considered the working reaction

$$NaSO_3Cl + OH \rightarrow NaHSO_4 + Cl, \qquad (e)$$

which does not break S–O bonds. The analogous potassium reactions were used for KSO_3 and KSO_3Cl. For each of the working reactions the reaction enthalpy was corrected to 298 K by means of $H_{298}-H_0$ for each species, to derive $\Delta_f H_{298}$ for the unknown molecules. The uncertainty in this method is at least equal to the propagated uncertainty of the thermochemistry of the reference molecules, which is on the order of ±10–15 kJ mol^{-1}.

4. Chemical kinetic model

The reaction mechanism developed in the present work consists of subsets for hydrogen/carbon monoxide oxidation, sulfur chemistry, chlorine chemistry, and potassium/sodium chemistry. The CO/H_2 [82] and S/H/O [83–86] subsets are drawn from earlier work. Of special interest are the reactions that oxidize SO_2 to SO_3, as they may be rate-limiting in formation of K_2SO_4. These reactions are discussed further below. The chlorine subset, which involves reactions of HCl and Cl_2, was drawn from the evaluation of Baulch et al. [87], except for a few reactions where more accurate data have become available.

Thermodynamic properties for selected alkaline species are listed in Appendix A and the reaction subset, in Appendix B. For the thermodynamic properties of sodium and potassium species we have supplemented data from the JANAF tables [81] and other evaluations [88,89] with recent high-level theoretical work [35–42] and calculations done in the present work. In addition to the alkaline metal–oxysulfur compounds discussed in the previous section, the entropies and heat capacities of NaO_2 and KO_2 were estimated in the present work.

The alkaline subset listed in Appendix B includes reactions of sodium and potassium with the O/H radical pool, with chlorinated species, and with sulfur oxides. It is intended for use under oxidizing conditions and does not include a number of reduced alkaline and alkali–sulfur species. Only a few of the rate constants in the Na/K/H/O/CO reaction subset have been determined experimentally. Most of the reactions were assigned estimated rate constants, but the present modeling predictions are not sensitive to the values. The interaction of sodium and chlorine species, primarily the reactions of Na, NaO, NaOH, and NaO_2 with HCl (or Cl_2) to form NaCl ((R31), (R32), (R33), (R35), (R36), (R38)), is fairly well established. These reactions have all been characterized experimentally [68,93,94], and with the exception of the endothermic step between Na and HCl to form NaCl and H, they are all very fast. In the potassium/chlorine subset, it is only the K + HCl (R81) reaction rate that has been measured [95]; we have estimated the other reactions in this subset by analogy with the corresponding sodium reactions.

Less is known about the interaction of alkaline species with sulfur compounds. To our knowledge only the recombination reactions of Na and K with SO_2 (R40), (R89) have been measured directly [34,80]; the rest of the reactions in this subset have estimated rate constants. Conceivably $NaSO_2$/KSO_2 behave similarly to NaO_2/KO_2: we expect them mainly to be recycled to SO_2 by dissociation or by reaction with O or OH. The recombination of Na and K with SO_3 to form $NaSO_3$/KSO_3 has been assigned high-pressure limiting rate constants corresponding to (R40) and (R89), respectively. QRRK theory was employed to estimate the low-pressure limiting rate constants. A second pathway to formation of $NaSO_3$/KSO_3, the reactions NaO + $SO_2(+M)$ = $NaSO_3(+M)$ (R43) and KO + $SO_2(+M)$ = KSO_3 $(+M)$ (R92), was also included in the mechanism. Scans of the HF/6-31G(d) potential energy surface for reaction (R43) indicate there is no barrier to addition, which is assumed for reaction (R92) as well. We expect $NaSO_3$/KSO_3 to be recycled largely to SO_3 by dissociation or by reaction with O/OH.

In the absence of measurements, the rate constants for reactions that form or consume $NaHSO_4$/$KHSO_4$ and $NaSO_3Cl$/KSO_3Cl have been estimated from

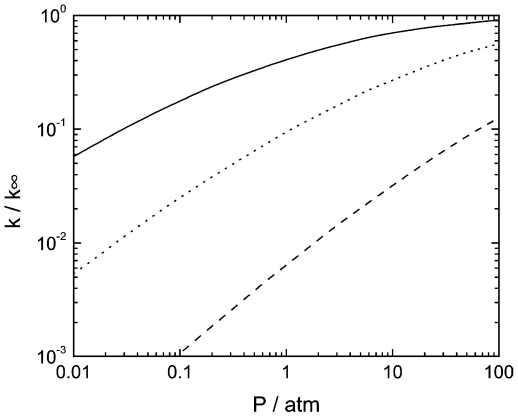

Fig. 2. Fall-off behavior of the reaction KOH + SO_3 = $KHSO_4$. From top to bottom, the data are at 1000 K (solid line), 1373 K (dotted line), and 2000 K (dashed line). From QRRK calculations we find that k_0(1000–2000 K) = $2.6 \times 10^{42} T^{-7.6}$ cm^6 mol^{-2} s^{-1}.

analogy with other reactions between polar species. For the reaction between KOH and SO_3,

$$KOH + SO_3(+M) = KHSO_4(+M), \quad (R93)$$

the rate coefficients were estimated from QRRK calculations, with an assumed high-pressure limit of 1×10^{14} cm^3 mol^{-1} s^{-1}. The similar reaction NaOH + $CO_2(+M)$ is very fast due to a strong attractive dipole to dipole-induced dipole interaction, with a high-pressure limit estimated to be approximately 4×10^{14} cm^3 mol^{-1} s^{-1} [65]. In support of the analogy between $AOH + CO_2(+M)$ and $AOH + SO_3(+M)$, calculations on the HF/6-31G(d) potential energy surface for NaOH + SO_3 show an attractive interaction at separations of several angstroms and no barrier to formation of the hydrogen sulfate adduct. Through consideration of microscopic reversibility, the A factor for the dissociation (R93b) was estimated to be 1.4×10^{17} s^{-1}. The fall-off behavior is shown in Fig. 2. At atmospheric pressure the reaction is at or near the high-pressure limit below 1000 K, while at higher temperatures fall-off effects are more significant. Preliminary QRRK results indicate a remarkably strong temperature dependence at the low-pressure limit, where k_{93} is proportional to T^{-n} with $n \approx 7$–8. This appears to arise in part from the rapidly increasing vibrational partition function of the adduct, which, in turn, reflects several low-frequency modes. For simplicity these have been treated as harmonic oscillators here; a more detailed analysis of anharmonic modes in alkali sulfates is planned in the future. The rate coefficients for the reaction

$$KCl + SO_3(+M) = KSO_3Cl(+M), \quad (R102)$$

were also derived this way. The reverse A factor is 5.3×10^{17} s^{-1} and the modest reaction enthalpy of −178 kJ mol^{-1} leads to smaller rate coefficients and third-order kinetics at atmospheric pressure and below.

The shuffle reactions involving $KHSO_4$ and KSO_3Cl,

$$KHSO_4 + KOH = K_2SO_4 + H_2O, \quad (R100)$$

$$KHSO_4 + KCl = K_2SO_4 + HCl, \quad (R101)$$

$$KSO_3Cl + H_2O = KHSO_4 + HCl, \quad (R104)$$

$$KSO_3Cl + KOH = K_2SO_4 + HCl, \quad (R105)$$

and the sodium analogs can be expected to exhibit ionic behavior and involve a comparatively strong collision complex, similar to reactions of alkali halides with other alkali halides or hydrogen halides. Rough estimates of the rate constants were made by analogy to the reaction between sodium hydroxide and hydrogen chloride,

$$NaOH + HCl = NaCl + H_2O. \quad (R36)$$

This exothermic reaction proceeds close to collision frequency (1.7×10^{14} cm^3 mol^{-1} s^{-1}) in the forward direction [68]. With the current thermodynamic properties the reverse reaction has a preexponential factor of about 10^{14} cm^3 mol^{-1} s^{-1} and an activation energy corresponding roughly to the endothermicity of the reaction. Consequently, we expect the shuffle reactions to be fast in the exothermic direction, and we assign them rate constants of 1×10^{14} cm^3 mol^{-1} s^{-1}. According to our present estimate for $\Delta_f H_{298}(KHSO_4)$ and $\Delta_f H_{298}(KSO_3Cl)$ the reactions that form K_2SO_4 (R100), (R101), (R105) are quite exothermic. These reactions, as well as the high-pressure limits for the association steps (R93) and (R102), can be assumed to be independent of temperature. A conservative, broad estimate of the uncertainty limits implies rate constants for these reactions in the range $1 \times 10^{13} \leqslant k \leqslant 5 \times 10^{14}$ cm^3 mol^{-1} s^{-1}. Reaction (R104) is exothermic by only 7 kJ mol^{-1}, i.e., basically thermoneutral within the uncertainty, and k_{104} has larger error limits as there may be a barrier to reaction.

In addition to alkaline species reactions, Appendix B includes a subset for SO_2/SO_3 interconversion, as this chemistry may have important implications for the alkali sulfation. This subset includes reactions of SO_2 with O (R1) and OH (R2), (R3) to form SO_3 either directly or through $HOSO_2$, as well as reactions that recycle SO_3 to SO_2 by reaction with O and SO (R4), (R5). All of these reactions, either in the forward or reverse direction, are potentially important for the SO_2/SO_3 ratio. For the $SO_2 + O(+M) = SO_3(+M)$ reaction (R1) we have adopted the rate coefficients determined very recently by Naidoo et al. [86]. The reaction $SO_2 + OH(+M) =$

$HOSO_2(+M)$ (R3) is equilibrated under the present conditions; the rate of SO_2 oxidation through $HOSO_2$ depends mainly on the thermodynamic properties for this species and the rate of its reaction with O_2. Among the other reactions that can contribute to SO_3 formation are $SO_2 + O_2 = SO_3 + O$ (R4b) and $SO_2 + SO_2 = SO_3 + SO$ (R5b). The rate constants for these reactions, which are both strongly endothermic, have been measured only in the reverse direction and they are associated with considerable uncertainties [83,84]. In the present work we rely on a flame measurement [90] for the rate of the $SO_3 + O$ reaction (R4); for $SO_3 + SO$ (R5) we adopt the room temperature measurement of Chung et al. [91] and estimate the temperature dependence to be similar to that of $SO + O_2 = SO_2 + O$.

5. Modeling of potassium sulfate formation

A significant problem in developing reliable reaction mechanisms for the high-temperature chemistry of alkali metals is the difficulties of obtaining accurate and well-characterized experimental data for kinetic modeling purposes. High temperature in situ diagnostics for alkali metals are limited mostly to the atomic form of the metal, and during cooling the metals are converted to condensable compounds that form deposits and/or aerosols, complicating chemical analysis. Often, alkali metal compounds must be introduced into the reaction system in liquid or particulate form and the vaporization process further complicates interpretation. For this reason many experiments on K or Na chemistry have been performed in flames [11,45,46,96,97] where the high temperatures facilitate complete vaporization (and subsequent dissociation) of the added alkali metals.

Unfortunately the reported flame studies are not suitable for our purposes. Most studies on alkali/sulfur interactions in flames are limited to the high-temperature regions, where alkali sulfate formation is not thermodynamically favored. To our knowledge, the only flame study to report alkali sulfate concentrations in the postflame zone is that of Stearns et al. [8]. However, Stearns et al. did not characterize the reaction conditions, in particular the temperature profile, in sufficient detail for kinetic modeling purposes.

In the present work we compare modeling predictions with the experimental data of Iisa et al. [47]. The experiments were conducted in a laminar entrained flow reactor, where small, solid particles (65–125 μm) of KCl were fed together with a gas consisting of SO_2, O_2, H_2O, and N_2. The experiments were performed at 1173–1373 K with residence times of 0.3–1.5 s in the hot reactor, followed by rapid cooling. In addition to temperature and residence time, the effect of $[O_2]$, $[SO_2]$, and $[H_2O]$ on the sulfation rate was investigated. The potassium chloride particles became molten in the hot zone and, depending on the temperature, 5–50% of the KCl(s) vaporized in the reactor. The gas-phase conversion of KCl to K_2SO_4 was determined from analysis of the amount and composition of the submicron particles collected on a filter downstream of the reactor. Sulfation of molten phase KCl was determined from analysis of the coarse particles captured in a cyclone. In good agreement with the results on the sulfation of NaCl particles at slightly lower temperatures [60], only a small fraction of the molten alkali chloride was sulfated.

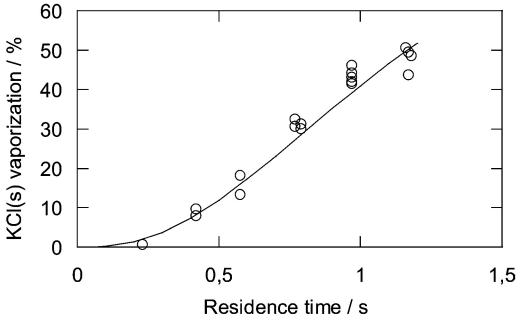

Fig. 3. Degree of vaporization of the solid KCl particles in the entrained flow reactor at 1373 K. Symbols denote experimental results [47]; solid line denotes predictions with a simplified vaporization model. KCl(s) feed, 0.24 g min^{-1}; total gas flow, 10–20 nL min^{-1}.

In the modeling we approximate the flow in the entrained flow reactor as plug flow and conduct the calculations with the SENKIN code [98], which runs in conjunction with the CHEMKIN package [99]. The evaporation of the solid potassium chloride is modeled as three pseudo-first-order reactions in series, with rate constants k', k'', and k''' fitted to obtain a match with the experimental data [47]. At 1373 K the best fit was obtained with $k' = k'' = k''' = 2.4$ s^{-1}. Fig. 3 compares the measured and predicted degree of vaporization of KCl(s) at this temperature as a function of residence time.

In the modeling we emphasize the results obtained at the highest temperature of 1373 K, where evaporation of the solid KCl is less likely to be a rate-limiting step in the sulfation process. However, even at this high temperature it is expected from equilibrium calculations that K_2SO_4 condenses to form aerosols. The equilibrium concentration of gas phase potassium sulfate under these conditions is only ≈ 10 ppm [47], a value far below the predicted K_2SO_4 formation if condensation is neglected. Because a detailed model of the nucleation and condensation process is outside the scope of the present work, we approximate the drain of potassium sulfate by condensation as a simple second-order reaction in $[K_2SO_4]$.

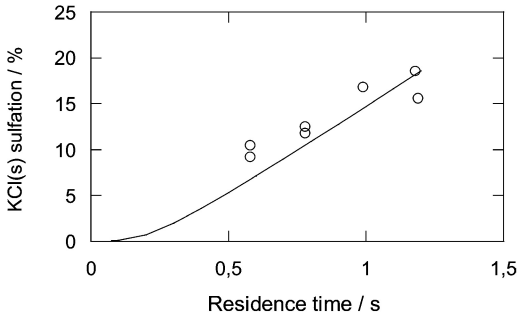

Fig. 4. Fractional conversion of solid KCl to K_2SO_4 as a function of residence time in an entrained flow reactor. Symbols denote experimental results [47]; solid line denotes modeling predictions. Experimental conditions: temperature, 1373 K; KCl(s) feed, 0.24 g min^{-1}; total gas flow, 10–20 nL min^{-1}; 2% SO_2, 5% O_2, 10% H_2O, balance N_2.

The rate constant for this pseudo-reaction was set to 10^{13} cm^3 mol^{-1} s^{-1}; this value prevents gaseous potassium sulfate from building up to concentrations above a few parts per million.

Chemical reaction in the cooling section following the hot isothermal zone might conceivably affect the partitioning of the alkali species. However, we assume that formation of K_2SO_4 during the rapid cooling is insignificant, as only small amounts of SO_3 would be available. Consequently, the total predicted formation of potassium sulfate formed in the reactor is taken as the sum of the gas-phase and condensed phase concentrations leaving the hot zone.

Fig. 4 compares the observed degree of sulfation of KCl in the entrained flow reactor as a function of the residence time at 1373 K [47] with modeling predictions. The inlet gas contained 2% SO_2, 5% O_2, and 10% H_2O. The results are shown as the fraction of the inlet (solid) potassium that is converted to potassium sulfate. Even though the model slightly underpredicts the potassium sulfate formation, the agreement between the modeling predictions, and the experimental results is remarkably good.

To identify the reactions, which according to the present model are important for the formation of potassium sulfate, sensitivity analysis, and rate-of-production analysis for the conditions of Fig. 4 were conducted. The present calculations support earlier suggestions [29,47] that oxidation of SO_2 to SO_3 is the rate-limiting step in the sulfation process. Under the conditions investigated the oxidation of SO_2 proceeds mainly through the sequence

$$SO_2 + OH(+M) = HOSO_2(+M), \quad (R3)$$

$$HOSO_2 + O_2 = SO_3 + HO_2. \quad (R6)$$

Minor contributions to formation of SO_3 come from direct oxidation reactions,

$$SO_2 + O(+M) = SO_3(+M), \quad (R1)$$

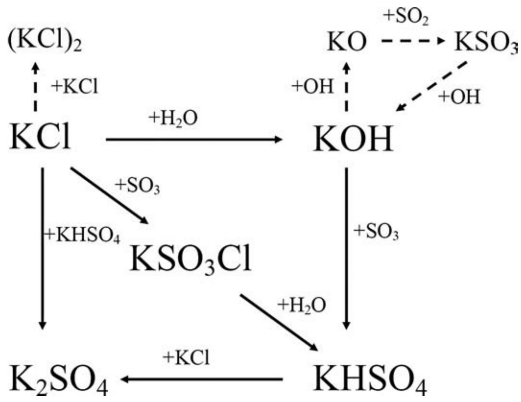

Fig. 5. Pathway diagram for potassium transformations under the conditions of Fig. 4.

$$SO_2 + OH = SO_3 + H, \quad (R2)$$

$$SO_2 + O_2 = SO_3 + O, \quad (R4b)$$

and from the reaction sequence,

$$SO_2 + KO(+M) = KSO_3(+M), \quad (R92)$$

$$KSO_3 + OH = SO_3 + KOH. \quad (R87)$$

Fig. 5 is a pathway diagram for the potassium transformations under the conditions of Fig. 4. Potassium chloride is the main form of gaseous potassium under the present conditions. After vaporization, KCl is partly converted to KOH by the reaction

$$KCl + H_2O = KOH + HCl. \quad (R85b)$$

In the early stage of reaction this is the major consumption step for KCl. As the SO_3 concentration builds up, KCl is converted mainly to KSO_3Cl:

$$KCl + SO_3(+M) = KSO_3Cl(+M). \quad (R102)$$

The KSO_3Cl complex reacts solely with H_2O, forming potassium hydrogen sulfate:

$$KSO_3Cl + H_2O = KHSO_4 + HCl. \quad (R104)$$

Potassium hydrogen sulfate is also formed by reaction of KOH with SO_3:

$$KOH + SO_3(+M) = KHSO_4(+M). \quad (R93)$$

According to the thermodynamic properties for KSO_3Cl and $KHSO_4$ estimated in the present work, both species are sufficiently stable in the gas phase at 1373 K to act as precursors for K_2SO_4. Potassium sulfate is formed by the K/H exchange reaction between $KHSO_4$ and KCl:

$$KHSO_4 + KCl = K_2SO_4 + HCl. \quad (R101)$$

Other potential routes to potassium sulfate, such as

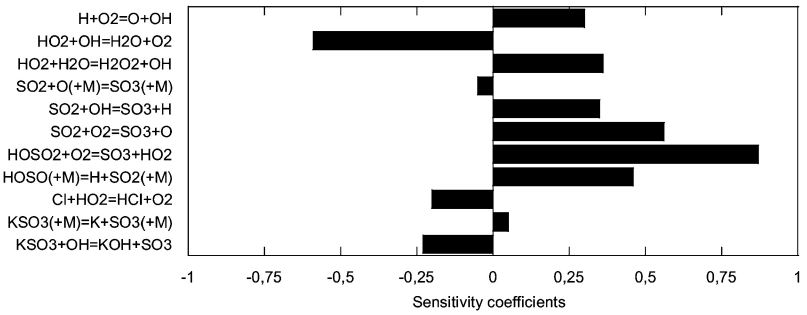

Fig. 6. First-order sensitivity coefficients for the elementary reactions with respect to formation of K_2SO_4 for conditions corresponding to Fig. 4 and a reaction time of 1.2 s. Reactions with sensitivity coefficients above 0.05 are listed.

$$KHSO_4 + KOH = K_2SO_4 + H_2O, \quad \text{(R100)}$$

$$KSO_3Cl + KOH = K_2SO_4 + HCl, \quad \text{(R105)}$$

are insignificant under the present conditions because KOH does not achieve concentrations above a few parts per million. Potassium chloride remains the dominant potassium species in the gas phase during the course of reaction; a minor part of the KCl recombines to form the $(KCl)_2$ dimer through reaction (R88).

Fig. 6 shows the results of a first-order sensitivity analysis of the predicted K_2SO_4 concentration with respect to the reaction rate constants for the conditions of Fig. 4. The analysis indicates that the sulfation rate is sensitive mainly to the reactions that generate or consume free radicals in the system. As no fuel is present to induce chain branching, reaction becomes very sensitive to generation of chain carriers; the availability of chain carriers governs the sulfur dioxide oxidation rate and thereby the rate of sulfation. The sulfation rate is enhanced by reactions that serve to replenish the radical pool, such as $H + O_2 = O + OH$ and $HO_2 + H_2O = H_2O_2 + OH$, and inhibited by chain-terminating reactions like $HO_2 + OH = H_2O + O_2$ and $Cl + HO_2 = HCl + O_2$. Even the reactions that oxidize SO_2 to SO_3 exhibit positive sensitivity coefficients only if they are chain propagating or chain branching. The reactions $SO_2 + OH = SO_3 + H$ (R2), $SO_2 + O_2 = SO_3 + O$ (R4b), and $HOSO_2 + O_2 = SO_3 + HO_2$ (R6) promote sulfation, whereas chain-terminating reactions such as $SO_2 + O(+M) = SO_3(+M)$ (R1) and $KSO_3 + OH = KOH + SO_3$ (R98) exhibit negative sensitivity coefficients even though they act to oxidize SO_2 to SO_3. Once formed, SO_3 reacts almost exclusively with potassium species, mainly KCl (R102) but also KOH (R93). The presence of potassium and particularly reaction (R102) increase the formation of SO_3 considerably. Under the conditions of Fig. 4 the rate of formation SO_3 in the absence of potassium is less than a third of the value with KCl present. It is, however, noteworthy, that neither (R102), (R93), nor the subsequent K/H/Cl exchange reactions that convert KSO_3Cl and $KHSO_4$ to K_2SO_4 show up in the sensitivity analysis.

The proposed sulfation mechanism involves intermediates and reactions, which have not been detected experimentally. It is of interest to evaluate how the uncertainty in the estimated properties in this subset affects the modeling predictions. According to our model the sulfation may occur either by the sequence $KCl \rightarrow KSO_3Cl \rightarrow KHSO_4 \rightarrow K_2SO_4$ (A) or by $KCl \rightarrow KOH \rightarrow KHSO_4 \rightarrow K_2SO_4$ (B). First we note that shutting off sequence (A) by removing KSO_3Cl from the mechanism has only a marginal impact on the predicted sulfation rate; sequence (B) is sufficient to explain the sulfate formation. Next we investigate the effect of the varying the heat of formation for $KHSO_4$ and the key rate constants in the subset on the K_2SO_4 prediction (Fig. 7). The upper part of Fig. 7 shows that even in the absence of KSO_3Cl in the model, a change in $\Delta_f H_{298}(KHSO_4)$ of more than 100 kJ mol^{-1} is required to cause a significant reduction in the predicted sulfation rate; this value is far beyond the estimated uncertainty limits of ± 15 kJ mol^{-1} in the ab initio calculations. The reactions selected for investigation were those forming and consuming $KHSO_4$ and KSO_3Cl, i.e., the association reactions ((R93) and (R102)) and the shuffle reactions ((R100), (R101), (R104), and (R105)). The lower part of Fig. 7 is based on calculations where the values of the rate constants for these reactions were systematically varied. Assuming all these reactions have the same rate constant (at the high-pressure limit), a reduction in the value of at least three orders of magnitude (in the absence of KSO_3Cl) was required to reduce the predicted sulfation rate by 50%. The fact that it requires drastic changes in the estimated properties to reduce or prevent gaseous sulfate formation in the calculations supports the credibility of the proposed model.

Fig. 8 shows the effect of the inlet SO_2 concentration on the sulfation of KCl at 1373 K. In this and the following figures, it is the fractional conversion

of the *vaporized* KCl that is shown. The experimental results show that even though sulfur dioxide in all experiments is present in considerable excess compared with the potassium concentration, the formation of K_2SO_4 increases significantly with the SO_2 level.

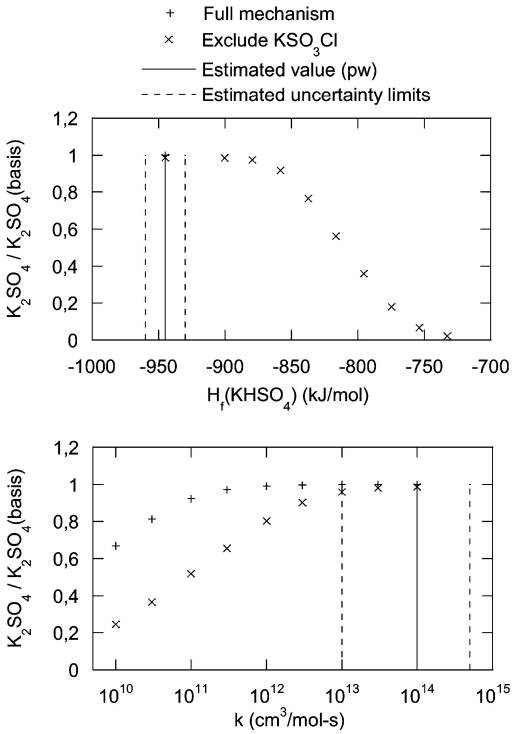

Fig. 7. Sensitivity of the predicted K_2SO_4 concentration to the heat of formation of $KHSO_4$ (top) and to selected rate constants ($k = k_{93,\infty} = k_{100} = k_{101} = k_{102,\infty} = k_{104} = k_{105}$) (bottom) for conditions corresponding to Fig. 4 and a reaction time of 1.2 s.

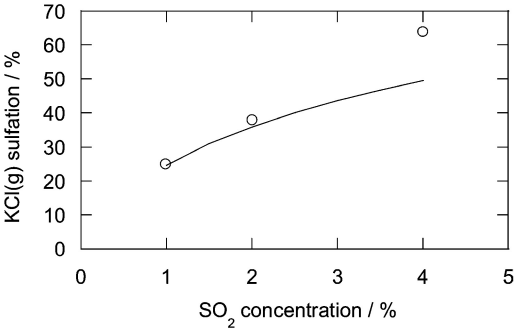

Fig. 8. Fractional conversion of vaporized KCl to K_2SO_4 as a function of the SO_2 concentration in an entrained flow reactor. Symbols denote experimental results [47]; solid line denotes modeling predictions. Experimental conditions: temperature, 1373 K; residence time, 1.2 s; KCl(s) feed, 0.24 g min^{-1}; total gas flow, 10–20 nL min^{-1}; 5% O_2, 10% H_2O, balance N_2.

This was taken to indicate that formation of SO_3 is a rate-limiting step in the sulfation process [47], in agreement with the present analysis. The modeling predictions are in good agreement with the experimental results, except at the highest SO_2 level, where the potassium sulfate formation is underpredicted. To predict the observed sulfation rate at 4% SO_2, the calculated oxidation rate for oxidation of SO_2 to SO_3 would have to increase substantially. The SO_2 oxidation rate is limited mainly by the availability of chain carriers, by the $SO_2/HOSO_2$ partial equilibrium, and by the rate of the $HOSO_2 + O_2$ reaction to form SO_3.

Fig. 9 shows the effect of the inlet O_2 concentration on K_2SO_4 formation. Even though the degree of sulfation is slightly underpredicted at the lowest oxygen level, the model captures the experimental trend

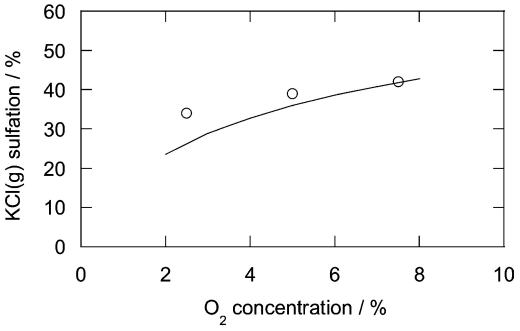

Fig. 9. Fractional conversion of vaporized KCl to K_2SO_4 as a function of the O_2 concentration in an entrained flow reactor. Symbols denote experimental results [47]; solid line denotes modeling predictions. Experimental conditions: temperature, 1373 K, residence time, 1.2 s; KCl(s) feed, 0.24 g min^{-1}; total gas flow, 10–20 nL min^{-1}; 2% SO_2, 10% H_2O, balance N_2.

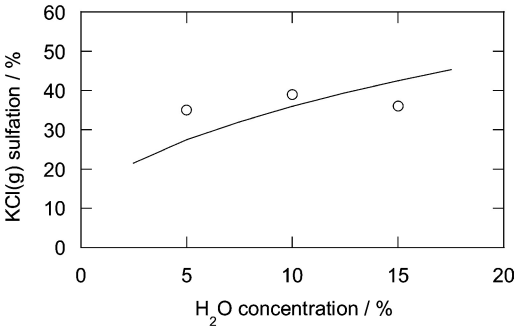

Fig. 10. Fractional conversion of vaporized KCl to K_2SO_4 as a function of H_2O concentration in an entrained flow reactor. Symbols denote experimental results [47]; solid line denotes modeling predictions. Experimental conditions: temperature, 1373 K; residence time, 1.2 s; KCl(s) feed, 0.24 g min^{-1}; total gas flow, 10–20 nL min^{-1}; 2% SO_2, 5% O_2, balance N_2.

well. The degree of sulfation increases with the oxygen level, but not as strongly as with the sulfur dioxide level. Fig. 10 shows the effect of the water vapor concentration. Here the experimental observations indicate that the sulfation rate is largely independent of $[H_2O]$, while the model predicts a significant increase in $[K_2SO_4]$ with increasing water vapor level. However, the discrepancy between the experimental data and the modeling predictions is probably within experimental uncertainty.

Without adjusting any parameters (except vaporization/condensation reactions) the present model offers a good estimate of potassium sulfate aerosol formation under the conditions investigated. The observed discrepancies may be explained by uncertainties in the SO_2-to-SO_3 oxidation chemistry, the interaction of potassium species with the O/H radical pool, and the simplified condensation/nucleation mechanism used in the model. Even though the present analysis and the model evaluation against the results of Iisa et al. [47] do not provide evidence for the proposed gas-phase sulfation mechanism, it appears plausible based on the estimated thermodynamic properties and the analogies with the class of alkali reactions that exhibits ionic behavior. There are alternative pathways to K_2SO_4, which may deserve further investigation. The first step in the sulfation process could be a reaction between SO_3 and an alkali chlorine dimer such as $(KCl)_2$; alkali hydroxide dimers are too unstable to be important at 1373 K. However, under the conditions investigated the degree of sulfation appears to be limited only by the SO_2 oxidation rate. This has the implication that the sulfation rate would be expected to be independent of the alkali precursor (KCl, KOH, NaCl, NaOH, or other).

Further validation of the mechanism will require comparison with experimental results over a wider range of conditions and alkali sulfate precursors. In particular, sulfate formation at lower temperatures should be investigated. However, to do this the model must be extended with a better description of the condensation and nucleation process that controls the drain of the sulfates out of the gas phase.

6. Conclusions

A detailed reaction mechanism for the sulfation of alkali metals is proposed. It describes the high-temperature gas-phase interaction between alkali metals, the O/H radical pool, and species of chlorine and sulfur. Thermodynamic properties of a number of potassium and sodium species, including alkali hydrogen sulfates and alkali oxysulfur chlorides, have been estimated from Gaussian 3 ab initio calculations. Rate constants have been drawn from the literature, from analogy with known reactions, or from QRRK theory. Sulfation is initiated by oxidation of SO_2 to SO_3. According to the model SO_3 subsequently recombines with alkali hydroxide or alkali chloride to form an alkali hydrogen sulfate or an alkali oxysulfur chloride. The ab initio calculations indicate that both of these complexes are sufficiently stable in the gas phase to act as precursors for alkali sulfate. Sulfation is completed by a number of shuffle reactions, which are all expected to be fast, although they involve stable molecules.

Modeling predictions compare favorably with the results from the entrained flow reactor experiments of Iisa et al. [47] on gas-phase sulfation of potassium chloride in a $SO_2/O_2/H_2O/N_2$ gas at 1373 K as a function of reaction time and gas composition. The predicted degree of sulfation is sensitive mainly to the rate oxidation of SO_2 and the production of chain carriers in the system, while the subsequent potassium transformations are too fast to be rate limiting.

Acknowledgments

The authors thank Hans Livbjerg, Flemming Frandsen, Anker Jensen, Jacob N. Knudsen, Mikko Hupa, and Arthur Fontijn for helpful discussions. P.G. acknowledges support from the CHEC (Combustion and Harmful Emission Control) Research Program and from PSO-Elkraft. P.M. thanks the National Science Foundation (Grant CTS-0113606), the Robert A. Welch Foundation (Grant B-1174), and the UNT Faculty Research Fund. Some of the calculations were performed at the National Center for Supercomputing Applications under Grant CHE000015N.

Appendix A
Thermodynamic properties for selected alkaline species[a]

Species	$H_{f,298}$	S_{298}	$C_{p,300}$	$C_{p,400}$	$C_{p,500}$	$C_{p,600}$	$C_{p,800}$	$C_{p,1000}$	$C_{p,1500}$	Source
Na	107.3	153.7	20.79	20.79	20.79	20.79	20.79	20.79	20.79	[81]
NaO	92.11	229.1	35.15	36.22	36.81	37.19	37.66	37.98	38.55	[35,81]
NaOH	−187.9	229.0	48.03	50.34	51.58	52.37	53.50	54.54	56.94	[38,88]
$(NaOH)_2$	−624.0	309.8	97.55	104.9	108.9	111.1	114.2	116.7	121.9	[88]
NaO_2	−46.0	257.5	47.47	50.40	52.39	53.77	55.44	56.34	57.33	[31,36], pw[b]

(continued on next page)

Appendix A (*continued*)

Species	$H_{f,298}$	S_{298}	$C_{p,300}$	$C_{p,400}$	$C_{p,500}$	$C_{p,600}$	$C_{p,800}$	$C_{p,1000}$	$C_{p,1500}$	Source
$NaSO_2$	−381.7	295.2	63.72	69.37	73.08	75.58	78.51	80.05	81.71	[80], pw
$NaSO_3$	−538.3	318.7	76.15	85.21	91.24	95.35	100.2	102.8	105.6	pw
$NaHSO_4$	−905.8	338.6	97.61	111.4	121.0	127.7	136.3	141.4	148.3	pw
Na_2SO_4	−1033.6	353.2	108.3	122.4	131.8	138.1	145.7	149.8	154.2	[81]
NaCl	−181.4	229.8	35.81	36.60	37.04	37.32	37.68	37.92	38.37	[81]
$(NaCl)_2$	−566.1	325.4	78.84	80.66	81.53	82.02	82.51	82.73	82.96	[81]
$NaSO_3Cl$	−742.7	346.8	94.77	105.2	112.2	117.1	123.0	126.2	129.8	pw
K	89.00	160.3	20.79	20.79	20.79	20.79	20.79	20.79	20.80	[81]
KO	55.18	238.0	35.98	36.78	37.22	37.51	37.91	38.19	38.76	[39,81]
KOH	−229.0	238.3	49.24	51.18	52.18	52.81	53.76	54.71	57.02	[41,89]
$(KOH)_2$	−641.0	342.9	105.7	110.1	112.4	113.7	115.7	117.7	122.3	[89]
KO_2	−67.0	268.7	48.32	50.85	52.64	53.92	55.51	56.38	57.34	[33,40], pw
KSO_2	−399.4	307.6	65.08	70.19	73.62	75.96	78.73	80.19	81.77	[34], pw
KSO_3	−563.9	330.5	77.14	85.76	91.58	95.57	100.3	102.9	105.7	pw
$KHSO_4$	−945.2	350.9	98.66	112.0	121.3	128.0	136.4	141.5	148.3	pw
K_2SO_4	−1094.1	379.2	110.2	123.5	132.5	138.6	146.0	149.9	154.2	[81]
KCl	−214.7	239.1	36.51	37.06	37.36	37.57	37.85	38.06	38.50	[81]
$(KCl)_2$	−617.6	352.9	80.89	81.86	82.31	82.57	82.82	82.93	83.05	[81]
KSO_3Cl	−788.6	361.2	97.19	106.5	112.9	117.5	123.2	126.3	129.8	pw

[a] Units are J, mol, K.
[b] pw, present work.

Appendix B
Reaction subset for alkaline species[a]

		A	n	E/R	
SO_2/SO_3 interconversion					
1.	$SO_2 + O(+M) = SO_3(+M)$	3.7E11	0.00	850	[86]
	Low-pressure limit	2.4E27	−3.60	2610	
	Troe parameters: 0.442 316 7442				
	Third-body efficiencies: $N_2 = 1.3$, $H_2O = 10$, $SO_2 = 10$				
2.	$SO_2 + OH = SO_3 + H$	4.9E02	2.69	12000	[83]
3.	$SO_2 + OH(+M) = HOSO_2(+M)$	7.2E12	0.00	360	[100]
	Low-pressure limit	4.5E25	−3.30	360	
	Troe parameters: 0.70 1E−30 1E30				
	Third-body efficiencies: $N_2 = 1.5$, $H_2O = 10$, $SO_2 = 10$				
4.	$SO_3 + O = SO_2 + O_2$	1.3E12	0.00	3070	[90]
5.	$SO_3 + SO = SO_2 + SO_2$	7.6E03	2.37	1500	[91], est[a]
6.	$HOSO_2 + O_2 = SO_3 + HO_2$	7.8E11	0.00	330	[101]
Na/H/O subsystem					
7.	$Na + O + M = NaO + M$	1.5E21	−1.50	0	[102], est[b]
8.	$Na + OH + M = NaOH + M$	5.4E21	−1.65	0	[43]
9.	$Na + HO_2 = NaOH + O$	1.0E14	0.00	0	[24], est
10.	$Na + HO_2 = NaO + OH$	3.0E13	0.00	0	est
11.	$Na + O_2(+M) = NaO_2(+M)$	3.6E14	0.00	0	[103]
	Low-pressure limit	6.6E21	−1.52	0	[92]
12.	$Na + H_2O_2 = NaOH + OH$	2.5E13	0.00	0	[68]
13.	$Na + H_2O_2 = NaO + H_2O$	1.6E13	0.00	0	[68]
14.	$NaO + H = Na + OH$	2.0E14	0.00	0	[24], est
15.	$NaO + O = Na + O_2$	2.6E14	0.00	0	[43,102]
16.	$NaO + OH = NaOH + O$	2.0E13	0.00	0	[24], est
17.	$NaO + HO_2 = NaOH + O_2$	5.0E13	0.00	0	[24], est
18.	$NaO + HO_2 = NaO_2 + OH$	5.0E13	0.00	0	[24], est
19.	$NaO + H_2 = NaOH + H$	1.6E13	0.00	0	[104]
20.	$NaO + H_2 = Na + H_2O$	3.1E12	0.00	0	[104][c]

(*continued on next page*)

Appendix B (*continued*)

		A	n	E/R	
21.	$NaO + H_2O = NaOH + OH$	1.3E14	0.00	0	[104]
22.	$NaO + CO = Na + CO_2$	1.3E14	0.00	0	[105]
23.	$NaOH + H = Na + H_2O$	5.0E13	0.00	0	est[d]
24.	$NaOH + NaOH = (NaOH)_2$	8.0E13	0.00	0	est as k_{39}
25.	$NaO_2 + H = Na + HO_2$	2.0E14	0.00	0	[24], est
26.	$NaO_2 + H = NaO + OH$	5.0E13	0.00	0	[24], est
27.	$NaO_2 + H = NaOH + O$	1.0E14	0.00	0	[24], est
28.	$NaO_2 + O = NaO + O_2$	1.3E13	0.00	0	[92]
29.	$NaO_2 + OH = NaOH + O_2$	2.0E13	0.00	0	[24], est
30.	$NaO_2 + CO = NaO + CO_2$	1.0E14	0.00	0	[24], est
Na/H/O/Cl subsystem					
31.	$Na + Cl + M = NaCl + M$	1.1E20	−1.00	0	[106], est
32.	$Na + HCl = NaCl + H$	1.3E15	0.00	5030	[94]
33.	$Na + Cl_2 = NaCl + Cl$	4.4E14	0.00	0	[107,108]
34.	$Na + ClO = NaCl + O$	1.0E14	0.00	0	est
35.	$NaO + HCl = NaCl + OH$	1.7E14	0.00	0	[68]
36.	$NaOH + HCl = NaCl + H_2O$	1.7E14	0.00	0	[68]
37.	$NaO_2 + Cl = NaCl + O_2$	1.0E14	0.00	0	est
38.	$NaO_2 + HCl = NaCl + HO_2$	1.4E14	0.00	0	[93]
39.	$NaCl + NaCl = (NaCl)_2$	8.0E13	0.00	0	[67]
Na/H/O/Cl/S subsystem					
40.	$Na + SO_2(+M) = NaSO_2(+M)$	1.2E14	0.00	0	[80]
	Low-pressure limit	2.0E23	−1.50	0	[80], est[b]
41.	$Na + SO_3(+M) = NaSO_3(+M)$	1.2E14	0.00	0	est as $k_{40,\infty}$
	Low-pressure limit[f]	1.4E35	−5.20	0	pw[f]
42.	$Na + SO_3 = NaO + SO_2$	1.0E14	0.00	10070	est[e]
43.	$NaO + SO_2(+M) = NaSO_3(+M)$	1.0E14	0.00	0	est as k_{40}
	Low-pressure limit	2.0E23	−1.50	0	
44.	$NaOH + SO_3(+M) = NaHSO_4(+M)$	1.0E14	0.00	0	est as k_{92}
	Low-pressure limit	2.6E42	−7.60	0	
45.	$NaSO_2 + O = NaO + SO_2$	1.3E13	0.00	0	est as k_{28}
46.	$NaSO_2 + OH = NaOH + SO_2$	2.0E13	0.00	0	est as k_{29}
47.	$NaSO_2 + NaO_2 = Na_2SO_4$	1.0E14	0.00	0	est
48.	$NaSO_3 + O = NaO + SO_3$	1.3E13	0.00	0	est as k_{28}
49.	$NaSO_3 + OH = NaOH + SO_3$	2.0E13	0.00	0	est as k_{29}
50.	$NaSO_3 + NaO = Na_2SO_4$	1.0E14	0.00	0	est
51.	$NaHSO_4 + NaOH = Na_2SO_4 + H_2O$	1.0E14	0.00	0	est[e]
52.	$NaHSO_4 + NaCl = Na_2SO_4 + HCl$	1.0E14	0.00	0	est[e]
53.	$NaCl + SO_3(+M) = NaSO_3Cl(+M)$	1.0E14	0.00	0	est as k_{102}
	Low-pressure limit	1.9E41	−7.80	0	
54.	$NaSO_3Cl + OH = NaHSO_4 + Cl$	1.0E14	0.00	0	est[e]
55.	$NaSO_3Cl + H_2O = NaHSO_4 + HCl$	1.0E14	0.00	0	est[e]
56.	$NaSO_3Cl + NaOH = Na_2SO_4 + HCl$	1.0E14	0.00	0	est[e]
K/H/O subsystem					
57.	$K + O + M = KO + M$	1.5E21	−1.50	0	est as k_7
58.	$K + OH + M = KOH + M$	5.4E21	−1.55	0	[43]
59.	$K + HO_2 = KOH + O$	1.0E14	0.00	0	est as k_9
60.	$K + HO_2 = KO + OH$	3.0E13	0.00	0	est
61.	$K + O_2(+M) = KO_2(+M)$	3.6E14	0.00	0	est as $k_{11,\infty}$
	Low-pressure limit	5.4E21	−1.32	0	[92]
62.	$K + H_2O_2 = KOH + OH$	2.5E13	0.00	0	est as k_{12}
63.	$K + H_2O_2 = KO + H_2O$	1.6E13	0.00	0	est as k_{13}
64.	$KO + H = K + OH$	2.0E14	0.00	0	est as k_{14}
65.	$KO + O = K + O_2$	2.2E14	0.00	0	est as k_{15}
66.	$KO + OH = KOH + O$	2.0E13	0.00	0	est as k_{16}

(*continued on next page*)

Appendix B (*continued*)

		A	n	E/R	
67.	$KO + HO_2 = KOH + O_2$	5.0E13	0.00	0	est as k_{17}
68.	$KO + H_2 = KOH + H$	1.6E13	0.00	0	est as k_{19}
69.	$KO + H_2 = K + H_2O$	3.1E12	0.00	0	est as k_{20}
70.	$KO + H_2O = KOH + OH$	1.3E14	0.00	0	est as k_{21}
71.	$KO + CO = K + CO_2$	1.0E14	0.00	0	est as k_{22}
72.	$KOH + H = K + H_2O$	5.0E13	0.00	0	est[d]
73.	$KOH + KOH = (KOH)_2$	8.0E13	0.00	0	est as k_{39}
74.	$KO_2 + H = K + HO_2$	2.0E14	0.00	0	est as k_{24}
75.	$KO_2 + H = KO + OH$	5.0E13	0.00	0	est as k_{25}
76.	$KO_2 + H = KOH + O$	1.0E14	0.00	0	est as k_{26}
77.	$KO_2 + O = KO + O_2$	1.3E13	0.00	0	est as k_{27}
78.	$KO_2 + OH = KOH + O_2$	2.0E13	0.00	0	est as k_{28}
79.	$KO_2 + CO = KO + CO_2$	1.0E14	0.00	0	est as k_{29}
K/H/O/Cl subsystem					
80.	$K + Cl + M = KCl + M$	1.8E20	−1.00	0	[106], est
81.	$K + HCl = KCl + H$	9.1E12	0.00	594	[95]
		1.0E14	0.00	1830	
	Duplicate reaction				
82.	$K + Cl_2 = KCl + Cl$	4.4E14	0.00	0	est as k_{32}
83.	$K + ClO = KCl + O$	1.0E14	0.00	0	est
84.	$KO + HCl = KCl + OH$	1.7E14	0.00	0	est as k_{34}
85.	$KOH + HCl = KCl + H_2O$	1.7E14	0.00	0	est as k_{35}
86.	$KO_2 + Cl = KCl + O_2$	1.0E14	0.00	0	est
87.	$KO_2 + HCl = KCl + HO_2$	1.4E14	0.00	0	est as k_{37}
88.	$KCl + KCl = (KCl)_2$	8.0E13	0.00	0	est as k_{38}
K/H/O/Cl/S subsystem					
89.	$K + SO_2(+M) = KSO_2(+M)$	3.7E14	0.00	0	[34]
	Low-pressure limit	5.2E23	−1.50	0	[34], est[b]
90.	$K + SO_3\ (+M) = KSO_3(+M)$	3.7E14	0.00	0	est as $k_{89,\infty}$
	Low-pressure limit	4.7E34	−4.90	0	pw[f]
91.	$K + SO_3 = KO + SO_2$	1.0E14	0.00	7840	est[e]
92.	$KO + SO_2(+M) = KSO_3(+M)$	3.7E14	0.00	0	est as k_{89}
	Low-pressure limit	5.2E23	−1.50	0	
93.	$KOH + SO_3(+M) = KHSO_4(+M)$	1.0E14	0.00	0	est
	Low-pressure limit	2.6E42	−7.6	0	pw[f]
94.	$KSO_2 + O = KO + SO_2$	1.3E13	0.00	0	est as k_{28}
95.	$KSO_2 + OH = KOH + SO_2$	2.0E13	0.00	0	est as k_{29}
96.	$KSO_2 + KO_2 = K_2SO_4$	1.0E14	0.00	0	est
97.	$KSO_3 + O = KO + SO_3$	1.3E13	0.00	0	est as k_{28}
98.	$KSO_3 + OH = KOH + SO_3$	2.0E13	0.00	0	est as k_{29}
99.	$KSO_3 + KO = K_2SO_4$	1.0E14	0.00	0	est
100.	$KHSO_4 + KOH = K_2SO_4 + H_2O$	1.0E14	0.00	0	est[e]
101.	$KHSO_4 + KCl = K_2SO_4 + HCl$	1.0E14	0.00	0	est[e]
102.	$KCl + SO_3(+M) = KSO_3Cl(+M)$	1.0E14	0.00	0	est
	Low-pressure limit	1.9E41	−7.80	0	pw[f]
103.	$KSO_3Cl + OH = KHSO_4 + Cl$	1.0E14	0.00	0	est[e]
104.	$KSO_3Cl + H_2O = KHSO_4 + HCl$	1.0E14	0.00	0	est[e]
105.	$KSO_3Cl + KOH = K_2SO_4 + HCl$	1.0E14	0.00	0	est[e]

[a] Temperature dependence estimated to be as for $SO + O_2 = SO_2 + O$ [84].
[b] Temperature exponent n estimated to be −1.5.
[c] Rate constant is lower limit.
[d] Estimated by analogy with $LiOH + H = Li + H_2O$ [109].
[e] Estimated with an A factor of 1×10^{14} cm^3 mol^{-1} s^{-1} and an activation energy corresponding to the endothermicity of the reaction.
[f] QRRK estimate (1000–2000 K).

References

[1] R. Friedman, J.R. Levy, Combust. Flame 7 (1963) 195–201.
[2] W.A. Rosser Jr., S.H. Inami, H. Wise, Combust. Flame 7 (1963) 107–119.
[3] J.D. Birchall, Combust. Flame 14 (1970) 85–96.
[4] K.S. Iya, S. Wollowitz, W.E. Kaskan, Proc. Combust. Inst. 15 (1974) 329–336.
[5] A. Cohen, L. Decker, Proc. Combust. Inst. 18 (1981) 225–231.
[6] G. Klingenberg, J.M. Heimerl, Prog. Astronaut. Aeronaut. 139 (1992) 241–260.
[7] V.I. Hanby, J. Eng. Power 96 (1974) 129–133.
[8] C.A. Stearns, R.A. Miller, F.J. Kohl, G.C. Fryburg, J. Electrochem. Soc. 124 (1977) 1145–1146.
[9] F.J. Kohl, G.J. Santoro, C.A. Stearns, D.E. Rosner, J. Electrochem. Soc. 126 (1979) 1054–1061.
[10] W.L. Fielder, C.A. Stearns, F.J. Kohl, J. Electrochem. Soc. 131 (1984) 2414–2417.
[11] M. Steinberg, K. Schofield, Prog. Energy Combust. Sci. 16 (1990) 311–317.
[12] M. Steinberg, K. Schofield, Proc. Combust. Inst. 26 (1996) 1835–1843.
[13] D.C. Dayton, R.J. French, T.A. Milne, Energy Fuels 9 (1995) 855–865.
[14] L.L. Baxter, T.R. Miles, T.R. Miles Jr., B.M. Jenkins, T. Milne, Dayton, R.W. Bryers, L.L. Oden, Fuel Process. Technol. 54 (1998) 47–78.
[15] H.P. Nielsen, L.L. Baxter, G. Sclippab, C. Morey, F.J. Frandsen, K. Dam-Johansen, Fuel 79 (2000) 131–139.
[16] L.A. Hansen, H.P. Nielsen, F.J. Frandsen, K. Dam-Johansen, S. Hørlyck, A. Karlsson, Fuel Process. Technol. 64 (2000) 189–209.
[17] W.D. Halstead, E. Raask, J. Inst. Fuel 42 (1969) 344–349.
[18] J.W. Hastie, E.R. Plante, D.W. Bonnell, ACS Symp. Ser. 179 (1982) 543–600.
[19] S. Srinivasachar, J.J. Helble, D.O. Ham, G. Domazetis, Prog. Energy Combust. Sci. 16 (1990) 303–309.
[20] S. Niksa, J. Helble, M. Harada, T. Ando, J. Shigeta, I. Kajigaya, Combust. Sci. Technol. 165 (2001) 229–247.
[21] D.C. Dayton, W.J. Frederick Jr., Energy Fuels 10 (1996) 284–292.
[22] L. Boonsongsup, K. Iisa, W.J. Frederick Jr., Ind. Eng. Chem. Res. 36 (1997) 4212–4216.
[23] J. Latva-Somppi, M. Moisio, E.L. Kauppinen, T. Valmari, P. Ahonen, J. Keskinen, J. Aerosol Sci. 29 (1998) 461–480.
[24] R.A. Perry, J.A. Miller, Int. J. Chem. Kinet. 28 (1996) 217–234.
[25] V.M. Zamansky, P.M. Maly, L. Ho, V.V. Lissianski, D. Rusli, W.C. Gardiner Jr., Proc. Combust. Inst. 27 (1998) 1443–1449.
[26] V.M. Zamansky, V.V. Lissianski, P.M. Maly, L. Ho, D. Rusli, W.C. Gardiner Jr., Combust. Flame 117 (1999) 821–831.
[27] V. Lissianski, V. Zamansky, G. Rizeq, Proc. Combust. Inst. 29 (2002) 2251–2258.
[28] K.A. Christensen, H. Livbjerg, Aerosol Sci. Technol. 25 (1996) 185–199.
[29] K.A. Christensen, M. Stenholm, H. Livbjerg, J. Aerosol Sci. 29 (1998) 421–444.
[30] J.R. Jensen, L.B. Nielsen, C. Schultz-Møller, S. Wedel, H. Livbjerg, Aerosol Sci. Technol. 33 (2000) 490–509.
[31] P. Marshall, A.S. Narayan, A. Fontijn, J. Phys. Chem. 94 (1990) 2998–3004.
[32] D.A. Horner, W.D. Allen, A.G. Csaszar, H.F. Schaefer III, Chem. Phys. Lett. 186 (1991) 346–355.
[33] H. Partridge, C.W. Bauschlischer Jr., M. Sodupe, S.R. Langhoff, Chem. Phys. Lett. 195 (1992) 200–206.
[34] A. Goumri, D. Laakso, J.-D. Rocha, E. Francis, P. Marshall, J. Phys. Chem. 97 (1993) 5295–5297.
[35] E.P.F. Lee, P. Soldan, T.G. Wright, Chem. Phys. Lett. 295 (1998) 354–358.
[36] E.P.F. Lee, P. Soldan, T.G. Wright, Chem. Phys. Lett. 301 (1999) 317–324.
[37] P. Soldan, E.P.F. Lee, S.D. Gamblin, T.G. Wright, Phys. Chem. Chem. Phys. 1 (1999) 4947–4954.
[38] E.P.F. Lee, T.G. Wright, J. Phys. Chem. A 106 (2002) 8903–8907.
[39] E.P.F. Lee, P. Soldan, T.G. Wright, J. Chem. Phys. 117 (2002) 8241–8247.
[40] E.P.F. Lee, T.G. Wright, Chem. Phys. Lett. 363 (2002) 139–143.
[41] E.P.F. Lee, T.G. Wright, Mol. Phys. 101 (2003) 405–412.
[42] M.B. Sullivan, M.A. Iron, P.C. Redfern, J.M.L. Martin, L.A. Curtiss, L. Radom, J. Phys. Chem. A 107 (2003) 5617–5630.
[43] D. Husain, J. Chem. Soc. Faraday Trans. 2 85 (1989) 85–130.
[44] J.M.C. Plane, in: A. Fontijn (Ed.), Gas-Phase Metal Reactions, Elsevier Science, Amsterdam, 1992, pp. 29–56.
[45] A.J. Hynes, M. Steinberg, K. Schofield, J. Chem. Phys. 80 (1984) 2585–2597.
[46] K. Schofield, M. Steinberg, J. Phys. Chem. 96 (1992) 715–726.
[47] K. Iisa, Y. Lu, K. Salmenoja, Energy Fuels 13 (1999) 1184–1190.
[48] R.A. Durie, J.W. Milne, M.Y. Smith, Combust. Flame 30 (1977) 221–230.
[49] M. Steinberg, K. Schofield, Combust. Flame 129 (2000) 453–470.
[50] P.J. Ficalora, O.M. Uy, D.W. Muenow, J.L. Margrave, J. Ceram. Soc. 51 (1968) 574–577.
[51] I. Eliezer, R.A. Howald, J. Chem. Phys. 65 (1976) 3053–3062.
[52] D. Cubiciotti, F.J. Keneshea, High. Temp. Sci. 4 (1972) 32–40.
[53] R.E. Fryxell, C.A. Trythall, R.J. Perkins, Corrosion 29 (1973) 423–428.
[54] J.C. Halle, K.H. Stern, J. Phys. Chem. 84 (1980) 1699–1704.
[55] K.H. Lau, R.D. Brittain, R.H. Lamoreaux, D.L. Hildenbrand, J. Electrochem. Soc. 132 (1985) 3041–3048.
[56] V. Sricharoenchaikul, W.J. Frederick Jr., T.M. Grace, J. Pulp Paper Sci. 23 (1997) 394–400.

[57] A.C. Cummings, The Manufacture of Hydrochloric Acid and Saltcake, Van Nostrand, New York, 1923.
[58] M. Henriksson, R. Warnqvist, Ind. Chem. Process Des. Dev. 18 (1979) 249–254.
[59] J.A.B. Satrio, S.B. Jagtap, T.D. Wheelock, Ind. Eng. Chem. Res. 41 (2002) 3540–3547.
[60] S. Ozawa, K. Ito, H. Matsuda, Kagaku Kogaku Ronbushu 28 (2002) 396–404.
[61] A.B. Anderson, N.C. Debnath, J. Phys. Chem. 87 (1983) 1938–1941.
[62] A.B. Anderson, J. Am. Chem. Soc. 106 (1984) 6262–6265.
[63] K.A. Christensen, H. Livbjerg, Aerosol Sci. Technol. 33 (2000) 470–489.
[64] D.R. Herschbach, Adv. Chem. Phys. 10 (1966) 319–393.
[65] J.W. Ager III, C.J. Howard, J. Geophys. Res. 92 (1987) 6675–6678.
[66] R.R. Herm, in: P. Davidovits, D.L. McFadden (Eds.), Alkali Halide Vapors, Academic Press, New York, 1979, Chapter 6.
[67] U. Alkemade, K.H. Homann, Ber. Bunsenges. Phys. Chem. 93 (1989) 434–439.
[68] J.A. Silver, A.C. Stanton, M.S. Zahniser, C.E. Kolb, J. Phys. Chem. 88 (1984) 3123–3129.
[69] W.B. Miller, S.A. Safron, D.R. Herschbach, J. Chem. Phys. 56 (1972) 3581–3592.
[70] M.J. Frisch, G.W. Trucks, H.B. Schlegel, G.E. Scuseria, M.A. Robb, J.R. Cheeseman, V.G. Zakrzewski, J.A. Montgomery Jr., R.E. Stratmann, J.C. Burant, S. Dapprich, J.M. Millam, A.D. Daniels, K.N. Kudin, M.C. Strain, O. Farkas, J. Tomasi, V. Barone, M. Cossi, R. Cammi, B. Mennucci, C. Pomelli, C. Adamo, S. Clifford, J. Ochterski, G.A. Petersson, P.Y. Ayala, Q. Cui, K. Morokuma, D.K. Malick, A.D. Rabuck, K. Raghavachari, J.B. Foresman, J. Cioslowski, J.V. Ortiz, A.G. Baboul, B.B. Stefanov, G. Liu, A. Liashenko, P. Piskorz, I. Komaromi, R. Gomperts, R.L. Martin, D.J. Fox, T. Keith, M.A. Al-Laham, C.Y. Peng, A. Nanayakkara, M. Challacombe, P.M.W. Gill, B. Johnson, W. Chen, M.W. Wong, J.L. Andres, C. Gonzalez, M. Head-Gordon, E.S. Replogle, J.A. Pople, GAUSSIAN 98, Revision A. 9, Gaussian, Inc., Pittsburgh, PA, 1998.
[71] M.J. Frisch, G.W. Trucks, H.B. Schlegel, G.E. Scuseria, M.A. Robb, J.R. Cheeseman, J.J.A. Montgomery, T. Vreven, K.N. Kudin, J.C. Burant, J.M. Millam, S.S. Iyengar, J. Tomasi, V. Barone, B. Mennucci, M. Cossi, G. Scalmani, N. Rega, G.A. Petersson, H. Nakatsuji, M. Hada, M. Ehara, K. Toyota, R. Fukuda, J. Hasegawa, M. Ishida, T. Nakajima, Y. Honda, O. Kitao, H. Nakai, M. Klene, X. Li, J.E. Knox, H.P. Hratchian, J.B. Cross, C. Adamo, J. Jaramillo, R. Gomperts, R.E. Stratmann, O. Yazyev, A.J. Austin, R. Cammi, C. Pomelli, J.W. Ochterski, P.Y. Ayala, K. Morokuma, G.A. Voth, P. Salvador, J.J. Dannenberg, V.G. Zakrzewski, S. Dapprich, A.D. Daniels, M.C. Strain, O. Farkas, D.K. Malick, A.D. Rabuck, K. Raghavachari, J.B. Foresman, J.V. Ortiz, Q. Cui, A.G. Baboul, S. Clifford, J. Cioslowski, B.B. Stefanov, G. Liu, A. Liashenko, P. Piskorz, I. Komaromi, R.L. Martin, D.J. Fox, T. Keith, M.A. Al-Laham, C.Y. Peng, A. Nanayakkara, M. Challacombe, P.M.W. Gill, B. Johnson, W. Chen, M.W. Wong, C. Gonzalez, J.A. Pople, GAUSSIAN 03, Gaussian, Inc., Pittsburgh, PA, 2003.
[72] L.A. Curtiss, K. Raghavachari, P.C. Redfern, V. Rassolov, J.A. Pople, J. Chem. Phys. 109 (1998) 7764–7776.
[73] L.A. Curtiss, P.C. Redfern, V. Rassolov, G. Kedziora, J.A. Pople, J. Chem. Phys. 114 (2001) 9287–9295.
[74] P.C. Hariharan, J.A. Pople, Chem. Phys. Lett. 16 (1972) 217–219.
[75] M.M. Francl, W.J. Pietro, W.J. Hehre, J.S. Binkley, M.S. Gordon, D.J. Defrees, J.A. Pople, J. Chem. Phys. 77 (1982) 3654–3665.
[76] V.A. Rassolov, M.A. Ratner, J.A. Pople, P.C. Redfern, L.A. Curtiss, J. Comput. Chem. 22 (2001) 976–984.
[77] F. Ramondo, L. Bencivenni, Mol. Phys. 67 (1989) 707–709.
[78] J.M.L. Martin, J. Chem. Phys. 108 (1998) 2791–2800.
[79] S.G. Lias, J.E. Bartmess, J.F. Liebman, J.L. Holmes, R.D. Levin, G.W. Mallard, Gas-Phase Ion, Neutral Thermochemistry, Am. Inst. of Physics, New York, 1988.
[80] Y. Shi, P. Marshall, J. Phys. Chem. 95 (1991) 1654–1658.
[81] M.W. Chase Jr., NIST-JANAF Tables, J. Phys. Chem. Ref. Data Monogr. 9 (1998), Am. Inst. of Phys., Am. Chem. Soc., New York, see also NIST Webbook http://webbook.nist.gov.
[82] P. Glarborg, M.U. Alzueta, K. Kjærgaard, K. Dam-Johansen, Combust. Flame 132 (2003) 629–638.
[83] P. Glarborg, D. Kubel, K. Dam-Johansen, H.-M. Chiang, J.W. Bozzelli, Int. J. Chem. Kinet. 28 (1996) 773–790.
[84] M.U. Alzueta, R. Bilbao, P. Glarborg, Combust. Flame 127 (2001) 2234–2251.
[85] P. Dagaut, F. Lecomte, J. Mieritz, P. Glarborg, Int. J. Chem. Kinet. 35 (2003) 564–575.
[86] J. Naidoo, A. Goumri, P. Marshall, Proc. Combust. Inst. (2003), in press.
[87] D.L. Baulch, J. Duxbury, S.J. Grant, D.C. Montague, Evaluated kinetic data for high temperature reactions. Vol. 4: Homogeneous gas phase reactions of halogen- and cyanide-containing species, J. Phys. Chem. Ref. Data Suppl. 10 (1981).
[88] L.V. Gurvich, G.A. Bergman, L.N. Gorokhov, V.S. Iorish, V.Ya. Leonidov, V.S. Yungman, J. Phys. Chem. Ref. Data 25 (1996) 1211–1276.
[89] L.V. Gurvich, G.A. Bergman, L.N. Gorokhov, V.S. Iorish, V.Ya. Leonidov, V.S. Yungman, J. Phys. Chem. Ref. Data 26 (1997) 1031–1110.
[90] O.I. Smith, S. Tseregounis, S.-N. Wang, Int. J. Chem. Kinet. 14 (1982) 679–697.
[91] K. Chung, J.G. Calvert, J.W. Bottenheim, Int. J. Chem. Kinet. 7 (1975) 161–182.
[92] M. Helmer, J.M.C. Plane, J. Geophys. Res. 98 (1993) 207–222.
[93] J.A. Silver, C.E. Kolb, J. Phys. Chem. 90 (1986) 3267–3269.
[94] J.M.C. Plane, B. Rajasekhar, L. Bartolotti, J. Chem. Phys. 91 (1989) 6177–6186.

[95] M. Helmer, J.M.C. Plane, J. Chem. Phys. 99 (1993) 7696–7702.

[96] C.P. Fenimore, Proc. Combust. Inst. 14 (1973) 955–963.

[97] D.E. Jensen, G.A. Jones, J. Chem. Soc. Faraday Trans. 1 78 (1982) 2843–2850.

[98] A. Lutz, R.J. Kee, J.A. Miller, Senkin: a Fortran program for predicting homogeneous gas-phase chemical kinetics with sensitivity analysis, Sandia Rep. SAND87-8248, Sandia National Laboratories, Livermore, CA, 1987.

[99] R.J. Kee, F.M. Rupley, J.A. Miller, Chemkin-II: a Fortran chemical kinetics package for the analysis of gas-phase chemical kinetics, Sandia Rep. SAND89-8009, Sandia National Laboratories, Livermore, CA, 1989.

[100] D. Fulle, H.F. Hamann, H. Hippler, Phys. Chem. Chem. Phys. 1 (1999) 2695–2702.

[101] R. Atkinson, D.L. Baulch, R.A. Cox, R.F. Hampson Jr., J.A. Kerr, M.J. Rossi, J. Troe, J. Phys. Chem. Ref. Data 26 (1997) 1329–1499.

[102] J. Griffin, D.R. Worsnop, R.C. Brown, C.E. Kolb, D.R. Herschbach, J. Phys. Chem. A 105 (2001) 1643–1648.

[103] W.B. DeMore, S.P. Sander, D.M. Golden, R.F. Hampson, M.J. Kurylo, C.J. Howard, A.R. Ravishankara, C.E. Kolb, M.J. Molina, Chemical Kinetics and Photochemical Data for Use in Stratospheric Modeling: Evaluation Number 12, 1997, JPL Publ. 97-4.

[104] J.W. Ager III, C.J. Howard, J. Chem. Phys. 87 (1987) 921–925.

[105] C.E. Kolb, D.R. Worsnop, M.S. Zahniser, G.N. Robinson, X. Shi, D.R. Herschbach, in: A. Fontijn (Ed.), Gas-Phase Metal Reactions, Elsevier Science, Amsterdam, 1992, pp. 15–27.

[106] D.E. Jensen, G.A. Jones, Combust. Flame 32 (1978) 1–34.

[107] J.A. Silver, J. Chem. Phys. 84 (1986) 4718–4720.

[108] C.L. Talcott, J.W. Ager III, C.J. Howard, J. Chem. Phys. 84 (1986) 6161–6169.

[109] J.M.C. Plane, B. Rajasekhar, J. Chem. Soc. Faraday Trans. 2 84 (1988) 273–285.